

Hole transport and carrier lifetime in InN epilayers

Fei Chen and A. N. Cartwright

Department of Electrical Engineering, The State University of New York, University at Buffalo, Buffalo, New York 14260

Hai Lu and William J. Schaff

Department of Electrical and Computer Engineering, Cornell University, Ithaca, New York 14853

(Received 25 July 2005; accepted 22 September 2005; published online 15 November 2005)

Time-resolved transient grating spectroscopy has been conducted to measure the ambipolar diffusion coefficient and to derive the hole mobility and carrier lifetime in an InN epilayer simultaneously. The ambipolar diffusion coefficient $D_a=2.0\text{ cm}^2/\text{s}$, hole mobility $\mu_h=39\text{ cm}^2/\text{V s}$, and carrier lifetime $\tau_R=5.4\text{ ns}$ at 300 K near the InN surface were determined by monitoring the transient grating kinetics at various grating periods. In addition, we observed a decrease of hole mobility and carrier lifetime at the internal epilayer/buffer interface in comparison with those at the free surface, suggesting a faster carrier capture rate to the defect states and a more efficient defect and impurity scattering mechanism. © 2005 American Institute of Physics.

[DOI: 10.1063/1.2133892]

The recent unexpected discovery¹⁻³ of the narrow band gap ($\sim 0.7\text{ eV}$) of InN, previously believed to be $\sim 1.9\text{ eV}$,⁴ has resulted in tremendous research attention because the reported high electron mobility, thermal and chemical stability, and small band gap makes this material very attractive for high-speed electronic devices, infrared emitters, solar cells, etc. In addition, this recent plethora of research activity has also led to significant debate about the origin of the observed emission and absorption.⁵ However, the narrow band gap is beginning to be more widely accepted and prospects for devices are beginning to be heavily investigated. In particular, the band gaps of $\text{In}_x\text{Ga}_{1-x}\text{N}$ ternary alloy system cover a very wide energy range from the infrared (InN) to the near ultra-violet (GaN), providing a perfect match with the solar energy spectrum.⁶ This provides an opportunity for the development and fabrication of new multijunction solar cells, which will have significantly improved efficiencies, and possibly reach the theoretically predicted ultimate efficiency for multijunction cells. Although extensive progress⁷⁻¹⁰ has been achieved regarding the growth, characterization, and simulation of InN, many device parameters and material properties are still lacking. One of the most important aspects for semiconductor devices is the carrier diffusivity. For instance, the diffusion length calculated by the mobility and carrier lifetime, determines the minority-carrier collection efficiency for a p - n junction, the key structure for a solar cell or a photodiode detector.

The Hall method has been commonly used to determine the electron mobility in InN.¹¹ The presence of a high unintentional n -type doping level in InN, however, makes this technique impractical for measuring the hole mobility as well as the hole diffusion length. The other traditional mobility measurement techniques include the time-of-flight techniques and various techniques to deduce the mobility from devices.¹² All of these techniques generally have relatively extensive sample preparation procedures, and some of these methods have very limited applicability. The time-resolved transient grating technique, on the other hand, was introduced as a direct method for carrier diffusivity determination. The technique is based on the formation of a photo-

generated carrier modulation (grating) by two interfering pulsed laser beams, and the detection of the diffraction of a third probe beam off this grating allows one to monitor the carrier diffusion dynamics.¹³⁻¹⁶ In this method, the simultaneous determination of hole mobility and carrier lifetime of InN is possible. It is worth mentioning that this technique is more accurate, and significantly more tedious, for measuring the carrier lifetime when compared to a transient transmission technique used in our previous papers.^{17,18}

In this letter, both the in-plane carrier transport and carrier lifetime at the free surface as well as at the epilayer/buffer interface of an InN epilayer were measured by time-resolved transient grating spectroscopy. This is the first direct measurement of ambipolar diffusion coefficient and hole mobility of InN. In addition, a slower hole mobility and a much shorter carrier lifetime was found near the InN/GaN interface with respect to those at the surface.

The epilayer studied in this work was a $5.5\text{ }\mu\text{m}$ InN film grown on a 200 nm GaN buffer layer that was deposited on a (0001) sapphire substrate by molecular beam epitaxy. The details of the growth technique have been reported elsewhere.¹⁰ The electron Hall mobility and free electron concentration were measured by Hall method as $2100\text{ cm}^2/\text{V s}$ and $3.7 \times 10^{17}\text{ cm}^{-3}$ at room temperature.

The transient grating experiments are performed at room temperature by using ultrafast laser pulses at 800 nm and $\sim 1.9\text{ }\mu\text{m}$ for grating writing and probing, respectively. Specifically, the laser source used is a Coherent regenerative amplifier (REGA), operating at 250 kHz . Part of the output of the REGA was frequency doubled to 400 nm to serve as the pump source for an optical parametric amplifier (OPA) that generates a tunable visible pulse (450 nm to 720 nm) and a tunable infrared pulse ($0.9\text{ }\mu\text{m}$ to $3.6\text{ }\mu\text{m}$) with typical pulse widths of $\sim 300\text{ fs}$. In these experiments, two coherent laser pulses from the REGA at 800 nm were focused onto the same spot on the sample. The direct absorption of the two interfering pump pulses created a thin free carrier grating with fringe spacing of $\Lambda = \lambda_{\text{pump}}/[2 \sin(\theta/2)]$, where θ is the angle between the two incident beams. The optical penetration depth estimated from the absorption coefficient (4.6

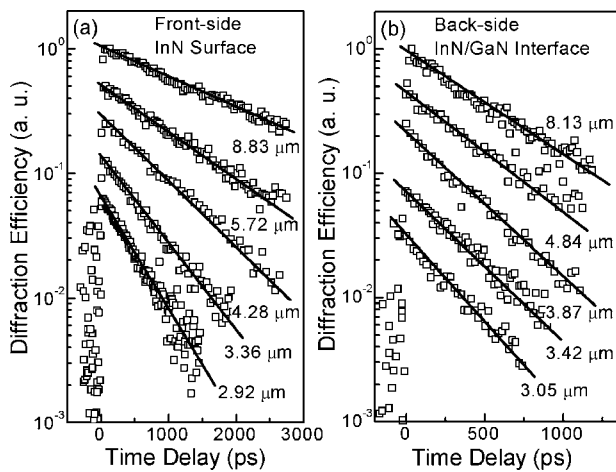


FIG. 1. The grating diffraction efficiency as a function of the probe delay time at the front side (a) and the back side (b) shown for different grating periods. Open circles show experimentally measured data. Solid lines indicate the single exponential fit.

$\times 10^4 \text{ cm}^{-1}$) for InN at the wavelength of 800 nm is about 220 nm. After pulsed excitation, the grating decays by both in-plane ambipolar diffusion and carrier recombination. A time-delayed infrared probe pulse at $\sim 1.9 \mu\text{m}$ from the OPA was focused onto the optically excited region of the sample to monitor electron-hole distribution as a function of time via the time-varying diffraction efficiency of the grating.

Due to the carrier induced changes in the absorption and refractive index, this carrier distribution forms a mixed amplitude-phase grating from which the probe can be diffracted. For the case of a thin sinusoidal grating, the temporal dependence of the diffraction efficiency can be written as¹⁹

$$\eta(t) = \frac{d^2}{4} \left[\left(\frac{\pi \Delta n_{p-p}}{\lambda_{\text{probe}}} \right)^2 + \left(\frac{\Delta \alpha_{p-p}}{4} \right)^2 \right] e^{-(2t/\tau_G)}, \quad (1)$$

where $\Delta \alpha_{p-p}$ and Δn_{p-p} refer to the peak to peak differences in the absorption and refractive index, d is the length of the active grating region, and τ_G is the grating decay rate. When assuming a monomolecular recombination, the decay rate τ_G is given by¹³⁻¹⁶

$$\frac{1}{\tau_G} = \frac{1}{\tau_R} + \frac{4\pi^2 D_a}{\Lambda^2}, \quad (2)$$

where τ_R is the carrier recombination lifetime, D_a is the ambipolar diffusion coefficient, and Λ is the grating period. The grating period can be adjusted by varying the angle θ between two pump beams. Thus, Eq. (2) indicates that the slope and the cross point to the axis of ordinate in a $1/\tau_G$ versus $4\pi^2/\Lambda^2$ plot directly provides the ambipolar diffusion coefficient and the reciprocal of the carrier lifetime, respectively.

As stated earlier, the measurements reported here were performed at both the front side and back side of the sample, to probe carrier diffusion and recombination dynamics near the surface and the InN/GaN interface. Figures 1(a) and 1(b) show the decay of the grating diffraction efficiency as a function of time delay for a set of different grating periods. The decay in each case exhibits a straight line on this semilogarithmic plot. Our previous papers^{17,18} have reported that the recombination mechanism at room temperature in such material is dominated by the defect related nonradiative recom-

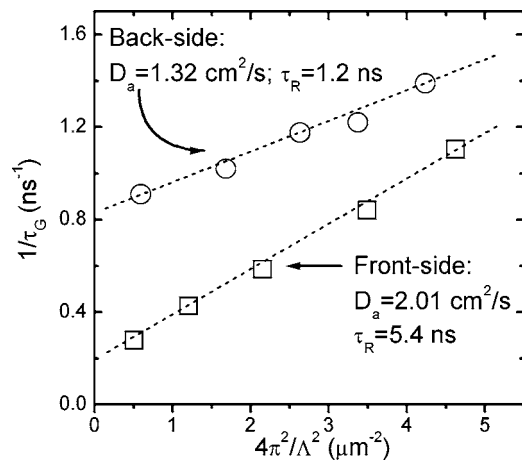


FIG. 2. Inverse grating decay time $1/\tau_G$ as a function of $4\pi^2/\Lambda^2$. Values of ambipolar diffusion coefficient, D_a , and recombination lifetime, τ_R , were obtained from the linear fit (dashed line) according to Eq. (2).

bination, rather than the bimolecular radiative and auger recombinations that generally cause a nonexponential decay in transient transmission signals. This hypothesis is further verified by the observed single exponential decay of the grating diffraction efficiency, as shown in Fig. 1. Since the grating decay rate is determined by both in-plane carrier diffusion and carrier recombination, the competition between these two processes produces a different result for the measurement at the front side and that at the back side of the InN layer. Specifically, we observed a significant decrease of τ_G at the surface as the grating period decreased as shown in Fig. 1(a), suggesting that the process is dominated by the in-plane carrier diffusion with a much slower recombination rate. On the other hand, only a slight change in the decay rate versus grating period near the back interface was observed as shown in Fig. 2(b), indicating a faster recombination rate with respect to the carrier diffusion.

As predicted in Eq. (2), and shown in Fig. 2, the plot of $1/\tau_G$ versus $4\pi^2/\Lambda^2$ is a straight line, where the slope determines the ambipolar diffusion coefficient and the intercept gives the reciprocal of the carrier lifetime. Thus, the ambipolar diffusion coefficient of 2.01 (1.32) cm^2/s and the carrier lifetime of 5.4 (1.2) ns for the surface (back interface) are extracted, respectively. Specifically, a decrease of carrier lifetime and diffusion coefficient from surface to the back interface is observed.

Physically, the significant difference between the effective electron and hole masses and mobilities results in ambipolar diffusivity. An electric field will develop due to the faster moving electrons with respect to the more slowly moving holes. This field will result in a coupling of the motion of the electrons and holes and results in a coupled diffusive motion. In the case of equal electron and hole densities, the ambipolar diffusion coefficient is determined in terms of the mobilities by²⁰

$$D_a = \frac{k_B T}{q} \left(\frac{2\mu_e \mu_h}{\mu_e + \mu_h} \right), \quad (3)$$

where k_B is the Boltzmann constant, q is the magnitude of the electronic charge, T is the carrier temperature, and μ_e and μ_h represent the electron and hole mobilities. Carrier mobility in a semiconductor can be calculated from $\mu = q\langle\tau\rangle/m^*$, where $\langle\tau\rangle$ is the average scattering and relaxation times and

m^* refers to the effective electron/hole masses. Due to a much heavier effective hole mass in InN, the electron mobility is assumed to be significantly larger than the hole mobility and thus Eq. (3) can be simplified as $D_a \approx 2k_B T \mu_h / q$, which enables us to directly estimate the hole mobility. Accordingly, the estimated hole mobility and the corresponding hole diffusion length, $L_h = \sqrt{(k_B T / q) \mu_h \tau_R}$, of the InN epilayer, was deduced as 39 cm²/V s and 0.74 μm near the free surface, and 26 cm²/V s and 0.28 μm near the interface.

The main contributions to the carrier scattering time include: (1) acoustic and optical phonon scattering; (2) impurity and defect scattering; (3) carrier-carrier scattering.²¹ The total scattering rate, whose inverse is a measure of the scattering time, can be measured by adding together all these individual rates for these scattering processes. The observed shorter carrier lifetime near the InN/GaN interface with respect to that at the surface suggests a faster carrier capture rate to the defect states, i.e., higher dislocation density near the internal interface. At the same time, a more efficient scattering of electrons and holes by defects and impurities may reduce the carrier mobility.

In conclusion, transient grating measurements have been used to determine the ambipolar diffusion coefficient, hole mobility, and carrier lifetime of an InN epilayer. A carrier lifetime of 5.4 ns and a hole mobility of 39 cm²/V s near the surface have been determined. The direct measurements of the hole mobility, carrier lifetime, as well as the resulting hole diffusion length, are essential for the development of InN based devices, particularly for high-efficiency solar cells.

This work was supported by the National Science Foundation CAREER Award, NSF No. 9733720, under the direction of Dr. Filbert Bartoli, and the Office of Naval Research Young Investigator Program Award No. N00014-00-1-0508 under the direction of Dr. Colin Wood. The work at Cornell University was supported by ONR under Contract No. N000149910936.

- ¹V. Y. Davydov, A. A. Klochikhin, R. P. Seisyan, V. V. Emtsev, S. V. Ivanov, F. Bechstedt, J. Furthmuller, H. Harima, A. V. Mudryi, J. Aderhold, O. Semchinova, and J. Graul, *Phys. Status Solidi B* **229**, R1 (2002).
- ²J. Wu, W. Walukiewicz, K. M. Yu, J. W. Ager III, E. E. Haller, H. Lu, W. J. Schaff, Y. Saito, and Y. Nanishi, *Appl. Phys. Lett.* **80**, 3967 (2002).
- ³T. Matsuoka, H. Okamoto, M. Nakao, H. Harima, and E. Kurimoto, *Appl. Phys. Lett.* **81**, 1246 (2002).
- ⁴T. L. Tansley and C. P. Foley, *J. Appl. Phys.* **59**, 3241 (1986).
- ⁵T. V. Shubina, S. V. Ivanov, V. N. Jmerik, D. D. Solnyshkov, V. A. Vekshin, P. S. Kopev, A. Vasson, J. Leymarie, A. Kavokin, H. Amano, K. Shimono, A. Kasic, and B. Monemar, *Phys. Rev. Lett.* **92**, 117407 (2004).
- ⁶J. Wu, W. Walukiewicz, K. M. Yu, J. W. Ager III, E. E. Haller, H. Lu, and W. J. Schaff, *Appl. Phys. Lett.* **80**, 4741 (2002).
- ⁷A. G. Bhuiyan, A. Hashimoto, and A. Yamamoto, *J. Appl. Phys.* **94**, 2779 (2003).
- ⁸V. Y. Davydov and A. A. Klochikhin, *Semiconductors* **38**, 861 (2004).
- ⁹I. Mahboob, T. D. Veal, C. F. McConville, H. Lu, and W. J. Schaff, *Phys. Rev. Lett.* **92**, No. 036804 (2004).
- ¹⁰W. J. Schaff, H. Lu, L. Eastman, W. Walukiewicz, K. M. Yu, S. Keller, S. Kurtz, B. Keyes, and L. Gevilas, in *The Electrochemical Society Proceedings Series*, edited by H. M. Ng and A. G. Baca (Electrochemical Society, New York, 2004), Vol. 2004-06, pp. 358-371.
- ¹¹D. C. Look, H. Lu, W. J. Schaff, J. Jasinski, and Z. Liliental-Webber, *Appl. Phys. Lett.* **80**, 258 (2002).
- ¹²D. K. Schroder, *Semiconductor Material and Device Characterization* (Wiley, New York, 1990), p. 194.
- ¹³V. Grivickas, V. Netiksis, D. Noreika, M. Petrauskas, M. Willander, M. A. Hasan, and W. X. Ni, *J. Appl. Phys.* **68**, 617 (1990).
- ¹⁴S. Komuro, A. Yoshinobu, S. Yusaburo, S. Namba, A. Masuyama, H. Okamoto, and Y. Hamakawa, *Appl. Phys. Lett.* **42**, 807 (1983).
- ¹⁵X. R. Huang, D. S. McCallum, M. D. Dawson, A. L. Smirl, T. F. Boggess, T. C. Hasenberg, and R. L. Tober, *J. Appl. Phys.* **74**, 1868 (1993).
- ¹⁶D. S. McCallum, A. N. Cartwright, X. R. Huang, T. F. Boggess, A. L. Smirl, and T. C. Hasenberg, *J. Appl. Phys.* **73**, 3860 (1993).
- ¹⁷F. Chen, A. N. Cartwright, H. Lu, and W. J. Schaff, *J. Cryst. Growth* **269**, 10 (2004).
- ¹⁸F. Chen, A. N. Cartwright, H. Lu, and W. J. Schaff, *Appl. Phys. Lett.* **83**, 4984 (2003).
- ¹⁹H. J. Eichler, P. Gunter, and D. W. Pohl, *Laser-Induced Dynamics Gratings* (Springer, Berlin, 1986).
- ²⁰K. Seeger, *Semiconductor Physics* (Springer, New York, 1985), p. 117.
- ²¹P. Y. Yu and M. Cardona, *Fundamentals of Semiconductors* (Springer, Berlin, 2001), p. 208.